

On the Mechanism of Air Pollutant Removal in
Two-Dimensional **Idealized** Street Canyons:
a Large-Eddy Simulation Approach

Tracy N. H. Chung and Chun-Ho Liu

Department of Mechanical Engineering, The University of Hong Kong, Hong Kong.

Revised manuscript
BOUN1124R1
submitted to
Boundary-Layer Meteorology
on
February 5, 2013.

**Corresponding author address:*

Chun-Ho LIU

Department of Mechanical Engineering

7/F, Haking Wong Building

The University of Hong Kong

Pokfulam Road, Hong Kong, CHINA

Tel: (852) 2859 7901

Fax: (852) 2858 5415

E-mail: liuchunho@graduate.hku.hk

On the Mechanism of Air Pollutant Removal in Two-Dimensional Idealized Street Canyons: a Large-Eddy Simulation Approach

Tracy N.H. Chung · Chun-Ho Liu

the date of receipt and acceptance should be inserted later

Abstract Flow resistance, ventilation, and pollutant removal for idealized two-dimensional (2D) street canyons of different building-height to street-width (aspect) ratios AR are examined using the friction factor f , air exchange rate (ACH), and pollutant exchange rate (PCH), respectively, calculated by large-eddy simulation (LES). The flows are basically classified into three characteristic regimes, namely isolated roughness, wake interference, and skimming flow, as functions of the aspect ratios. The LES results are validated by various experimental and numerical datasets available in the literature. The friction factor increases with decreasing aspect ratio and reaches a peak at $AR = 0.1$ in the isolated roughness regime and decreases thereafter. As with the friction factor, the ACH increases with decreasing aspect ratio in the wake interference and skimming flow regimes, signifying the improved aged air removal for a wider street canyon. The PCH exhibits a behaviour different from its ACH counterpart in the range of aspect ratios

Department of Mechanical Engineering, The University of Hong Kong, Pokfulam Road, Hong Kong

tested. Pollutants are most effectively removed from the street canyon **with** $AR = 0.5$. However, a minimum of PCH is found nearby at $AR = 0.3$, at which the pollutant removal is sharply weakened. Besides, the ACH and PCH are partitioned into the mean and turbulent components to compare their relative contributions. In line with our **earlier** Reynolds-averaged Navier-Stokes **calculations (Liu et al. 2011)**, the current LES shows that the turbulent components contribute more to both ACH and PCH, consistently demonstrating the importance of atmospheric turbulence in the ventilation and pollutant removal for urban areas.

Keywords: Air quality, City ventilation, Large-eddy simulation, Pollutant removal, Urban areas.

1 Introduction

In view of the growth of urbanization and population in the current era, urban air quality has been an important research topic for years (Britter and Hanna 2003; Vardoulakis et al. 2003; Ahmad et al. 2005). Apart from three-dimensional (3D) cubes (Coceal et al. 2006; Kanda 2006), **a** street canyon is the basic unit constructing a city, **and** a fundamental understanding of the transport processes **within the street canyon**, helps elucidate the ventilation, as well as promote pollutant removal from **the** ground to the urban boundary layer (UBL) **above** (Liu and Barth 2002).

Because of the similarity of heat and mass transport, hot ribs have been employed to study the forced heat transfer over rough surfaces. Chow (1959) introduced k -type and d -type flows to characterize the flow over repeated ribs placed

12 in a cross flow. Analogously, idealized two-dimensional (2D) street canyons are
13 commonly used in urban climate research. Their building-height to street-width
14 (aspect) ratio AR is the key parameter defining the building geometry and the flow
15 patterns. Oke (1988) characterized the flows in street canyons into three regimes,
16 namely isolated roughness ($AR < 0.3$, wide street), wake interference ($0.3 \leq AR$
17 ≤ 0.7), and skimming flow ($0.7 < AR$, tall buildings). It is found that k -type flows
18 are distinguished by flow re-attachment and separation between the ribs. These
19 flow characteristics are in line with the prevailing entrainment of air in the isolated
20 roughness regime (Jiménez 2004). Similar to d -type flows, a dividing streamline
21 bridges the top of leeward and windward ribs in which the recirculating flows are
22 isolated from the flow aloft in the skimming flow regime (Belcher 2005). Bottema
23 (1997) proposed the correlation between roughness and transport processes but
24 this was difficult to quantify. These flow characteristics explain the retention and
25 re-entrainment of pollutants in 2D street canyons in the wake interference regime
26 (Liu et al. 2011).

27 The urban climate community is increasingly interested in the skimming flow
28 regime because of the closely packed nature of buildings in a city. A series of
29 studies have been performed in the Department of Mechanical Engineering, the
30 University of Hong Kong to examine the ground-level air quality as a function
31 of street-canyon geometry. The concept of air exchange rate (ACH) and pollu-
32 tant exchange rate (PCH) was proposed by Liu et al. (2005) to quantify the air
33 quality in street canyons using large-eddy simulation (LES). While LES is compu-
34 tationally more demanding, Li et al. (2005) later used the renormalisation group
35 (RNG) k - ϵ turbulence model to formulate the ACH for Reynolds-averaged Navier-

36 Stokes (RANS) applications. Recently, Cheng et al. (2008) extended the RANS
37 formulation to calculate PCH. These studies have presented two simple indicators
38 measuring the performance of ventilation and pollutant removal for **idealized** 2D
39 street canyons in various configurations, such as high-rise buildings (Li et al. 2009)
40 or in unstable thermal stratification (Cheng and Liu 2011*b*).

41 One of the major merits of ACH and PCH is the partitioning of transport pro-
42 cesses into their mean and turbulent components. Applying LES to street canyons
43 **with** unity aspect ratio in the skimming flow regime, Cheng and Liu (2011*a*)
44 demonstrated that both ventilation and pollutant removal are largely governed
45 by intermittency. On the other hand, a comprehensive RANS k - ϵ turbulence mod-
46 elling study was conducted by Liu et al. (2011) in which the ACH and PCH for a
47 wide range of aspect ratio were calculated to cover all the flow regimes. The most
48 interesting finding is the dissimilar **behaviours** of ACH and PCH as functions of
49 aspect ratio, suggesting the necessity of using both indicators simultaneously to
50 measure ground-level ventilation and air quality. Apart from the dominant turbu-
51 lent pollutant removal from street canyons to the UBL, pollutant re-entrainment,
52 which drives roof-level pollutants **downwards** into the street canyon, was revealed.
53 The RANS results showed that the pollutant re-entrainment is governed by the
54 persistent entrainment **of air** via mean PCH, resulting in the prolonged pollutant
55 retention.

56 The pollutant removal mechanism for **idealized** 2D street canyons has been
57 primarily formulated after the aforementioned studies. However, the weaknesses
58 of RANS k - ϵ turbulence models, handling flow separation, re-attachment, and re-
59 circulation, might affect the modelling accuracy of transport processes. Previous

60 LESs have often overlooked the processes in isolated roughness and wake interfer-
61 ence regimes because of the major concern of compact buildings in urban areas
62 (Cui et al. 2004; Letzel et al. 2008; Gu et al. 2011; Michioka et al. 2011). Moreover,
63 the roof-level intermittent transport processes calculated by RANS k - ϵ turbulence
64 models could be prone to error under strong anisotropic shear. This study is thus
65 conceived, using the more sophisticated LES, to investigate the ventilation and
66 pollutant removal in all flow regimes for idealized 2D street canyons. In particular,
67 we attempt to demystify the mechanism of pollutant re-entrainment, which is sig-
68 nified by a negative mean PCH, by calculating the transient, large-energy-carrying
69 scales explicitly.

70 Our core objective is to contrast the characteristic ventilation and pollutant
71 removal in idealized 2D street canyons with different aspect ratios ($0.0667 \leq AR \leq$
72 2) covering the three major flow regimes. Further to the RANS results of Liu et al.
73 (2011), the mean and turbulent ACH and PCH calculated by the current LES
74 are analyzed to elucidate the role of atmospheric turbulence in pollutant removal
75 from urban areas. Finally, as a pilot trial, the correlation among ACH, PCH, and
76 the friction factor is investigated to determine whether the flow resistance over
77 hypothetical urban areas could serve as an appropriate indicator of city ventilation
78 and pollutant removal.

79 2 Methodology

80 Computational fluid dynamics (CFD) is employed to calculate the wind and pol-
81 lutant transport in idealized 2D street canyons of various aspect ratios. The LES

82 with the one-equation subgrid-scale (SGS) model of the open-source CFD code
 83 OpenFOAM 1.6 (OpenFOAM 2012) is used. The mathematical model and the
 84 governing equations are detailed below.

85 2.1 Governing Equations

86 The incompressible Navier-Stokes equations in isothermal conditions are employed,
 87 **which** consist of the continuity equation

$$\frac{\partial \bar{u}_i}{\partial x_i} = 0 \quad (1)$$

88 and the momentum conservation **equation**

$$\frac{\partial \bar{u}_i}{\partial t} + \frac{\partial}{\partial x_j} \bar{u}_i \bar{u}_j = -\Delta P_x \delta_{i1} - \frac{\partial \bar{\pi}}{\partial x_i} + \nu \frac{\partial^2 \bar{u}_i}{\partial x_j \partial x_j} - \frac{\partial \tau_{ij}}{\partial x_j}. \quad (2)$$

89 Here, \bar{u}_i are the resolved-scale velocity tensors in the i -directions, x_i **are** the Carte-
 90 sian coordinates, ΔP_x **is** the background pressure gradient in streamwise direction,
 91 δ_{ij} **is** the Kronecker delta, and ν **is** the kinematic viscosity. The modified resolved-
 92 scale pressure is

$$\bar{\pi} = \bar{p} + \frac{2}{3} k_{SGS} \quad (3)$$

93 where \bar{p} is the resolved-scale kinematic pressure and k_{SGS} **is** the SGS turbulent
 94 kinetic energy (TKE). The SGS Reynolds stresses $-\tau_{ij}$ ($= -[\bar{u}_i \bar{u}_j - \bar{u}_i \bar{u}_j]$) are
 95 modelled in the form

$$-\tau_{ij} = \nu_{SGS} \left(\frac{\partial \bar{u}_i}{\partial x_j} + \frac{\partial \bar{u}_j}{\partial x_i} \right) + \frac{2}{3} k_{SGS} \delta_{ij} \quad (4)$$

96 using the Smagorinsky SGS model (Smagorinsky 1963). Here, ν_{SGS} ($= C_k k_{SGS}^{1/2} \Delta$)
 97 is the SGS kinematic viscosity, Δ ($= [\Delta_x \Delta_y \Delta_z]^{1/3}$) **is** the filter width, and C_k ($=$

98 0.07) is an empirical modelling constant. The mass conservation is calculated by
 99 the advection-diffusion equation for a passive and inert pollutant

$$\frac{\partial \bar{\phi}}{\partial t} + \bar{u}_i \frac{\partial \bar{\phi}}{\partial x_i} = \kappa \frac{\partial^2 \bar{\phi}}{\partial x_i \partial x_i} - \frac{\partial \sigma_i}{\partial x_i} \quad (5)$$

100 where $\bar{\phi}$ is the resolved-scale pollutant concentration and κ is the mass diffusivity.

101 Analogous to Reynolds stresses, the SGS pollutant fluxes $\sigma_i (= [\overline{\phi u_i} - \bar{\phi} \bar{u}_i])$ are

102 modelled by gradient diffusion

$$\sigma_i = -\kappa_{SGS} \frac{\partial \bar{\phi}}{\partial x_i} \quad (6)$$

103 where $\kappa_{SGS} (= \nu_{SGS}/Sc)$ is the SGS mass diffusivity and $Sc (= 0.72)$ is the

104 Schmidt number.

105 2.2 Computational Domain and Boundary Conditions

106 A 3D computational domain of height $6h$ is used for the LES (Fig. 1). As with

107 Cai et al. (2008), the spatial domain consists of a pair of hypothetical leeward

108 and windward buildings of equal height h , and an open channel of depth $5h$. An

109 idealized unit of a 2D street canyon is constructed by extending the open channel

110 by $h/2$ horizontally over both the upstream and downstream buildings. Given a

111 constant building height h , the street width b between the leeward and windward

112 buildings is the sole parameter controlling the aspect ratios. The computational

113 domain is of size $5h$ in the homogeneous spanwise direction (with the same building

114 geometry) in which the properties are averaged to calculate the ensemble average

115 in the analysis. The flow aloft, which is driven by the pressure gradient ΔP_x in

116 the open channel, is aligned perpendicular to the street axis, representing the

117 worst scenario for pollutant removal. The infinitely long and infinitely repeating
118 street canyons are simulated using cyclic boundaries in the horizontal directions.
119 No-slip conditions ($\bar{u}_i = 0$) are applied to the solid boundaries, while the domain
120 top is assumed to be shear free ($\partial\bar{u}/\partial z = \partial\bar{v}/\partial z = \bar{w} = 0$). All the solid bound-
121 aries, including the leeward and windward facades, building tops, and streets, are
122 prescribed at a uniform pollutant concentration Φ . Unlike the cyclic boundaries
123 employed in the flow, a zero-pollutant inflow and an open-boundary condition are
124 applied at the upstream inflow and downstream outflow, respectively. In the span-
125 wise direction, the pollutant boundary condition is assumed to be cyclic similar
126 to its flow counterpart.

127 2.3 Numerical Method

128 In the current LES, the implicit second-order accurate backward differencing is
129 used in the time integration. The second-order accurate Gaussian finite volume
130 method (FVM) is adopted to calculate the gradient, divergence, and Laplacian
131 terms. The spatial domain is discretized into different **numbers** of elements (6.5
132 $\times 10^6$ to 8×10^6) depending on the **aspect ratio**. The first element is placed at
133 around **five** wall units measured from the nearby solid boundary to resolve the
134 near-wall flows. The Reynolds number $Re (= \bar{U}h/\nu)$ based on the mean flow speed
135 \bar{U} (calculated by the average value in the vertical direction) and the building height
136 is in the range of 1.10×10^5 to 1.27×10^5 , **which** is high enough for flows **to be**
137 independent **of** molecular viscosity.

138 3 Results and Discussion

139 We focus on the relation between the aerodynamic resistance, and the rates of
 140 ventilation and pollutant removal along the opening gap of street canyons. Their
 141 behaviour in different flow regimes is discussed in this section. In the analysis,
 142 angular parentheses $\langle \cdot \rangle$ represent the ensemble-averaged LES properties in the
 143 temporal domain and the homogeneous spanwise direction. Instead of the velocity
 144 scale, the friction factor f is used to describe the kinematic effects, while the
 145 ACH and PCH are used to measure the ventilation and the pollutant removal,
 146 respectively. It is noteworthy that several other indicators, such as the exponential
 147 decay time constant (Lee and Park 1994), the integral dilution time scale (Sini et al.
 148 2005), the pollutant transfer coefficient (Barlow and Belcher 2002), the pollutant
 149 exchange velocity (Bentham and Britter 2003), the wall transfer velocity (Narita
 150 2007), the purging flow rate, the visitation frequency, and the residence time (Bady
 151 et al. 2008), are also commonly used to measure the air quality in a street canyon.

152 3.1 Friction Factor

153 The Darcy-Weisbach equation (Munson et al. 2009) depicts the head loss due to
 154 the skin friction along a given length of pipe as a function of flow properties.
 155 The loss in kinematic pressure Δp can be expressed as a function of the channel
 156 length L , mean flow speed \bar{U} , friction factor f , and hydraulic diameter D_h ($=$
 157 $2WH/(W+H)$) for a rectangular channel of width W and height H , as follows

$$\Delta p = f \left(\frac{L}{D_h} \right) \left(\frac{\bar{U}^2}{2} \right). \quad (7)$$

158 Re-ordering Eq. 7 yields

$$f = \frac{\Delta p D_h / L}{(\overline{U^2} / 2)} = \frac{\tau_w}{(\rho \overline{U^2} / 2)}, \quad (8)$$

159 so **that** the friction factor f can be defined as the ratio of **the** shear stress τ_w (=
 160 $\rho \Delta p D_h / L$, where ρ is the fluid density) to **the** mean kinetic energy per unit volume.
 161 It also represents the pressure difference required to sustain a flow against the flow
 162 resistance.

163 Figure 2a shows the LES friction factor calculated by Eq. 8. The shear stress
 164 is calculated by the force balance in the UBL $\tau_w = \rho \Delta P_x \times 5h$. Also shown are the
 165 measurements (Han 1984) and the RANS $k-\epsilon$ turbulence model results (Liu et al.
 166 2011). Han (1984) measured the flow resistance over 2D ribs placed in **a** cross flow
 167 in a rectangular channel. The current LES overpredicts slightly compared with the
 168 measurements in the isolated roughness regime, **which could be due** to the different
 169 methods **used to measure** the pressure difference across the test section. In the
 170 wake interference and part of the skimming flow regimes, the trend of the modelling
 171 results **is** consistent with each other, **although** the experimental measurements of
 172 Han (1984) **did** not extend to high aspect ratios. The laboratory measurements
 173 and modelling results collectively suggest that the friction factor **peaks** at around
 174 $AR = 0.125$ and **decreases** thereafter with decreasing aspect ratio.

175 In the isolated roughness regime, the LES shows that the friction factor de-
 176 creases nearly monotonically with decreasing aspect ratio, i.e., the wider the street,
 177 the lower is the flow resistance. The flows are characterized by the persistent air
 178 entrainment down to ground level and the subsequent flow separation on the wind-
 179 ward side. The decreasing resistance is attributed to the wider building separation

180 and the smaller shear drag over the smooth ground surface (compared to the form
181 drag due to the impingement on the building facades), resulting in the reduced
182 overall flow resistance across a basic unit of street canyon.

183 Further reducing the street width switches the flow from the isolated rough-
184 ness to the wake interference regimes in which the friction factor decreases with
185 increasing aspect ratio. Different from the flow in the isolated roughness regime,
186 the prevailing air masses do not touch down on the ground surface. The flow only
187 partly entrains into the upper street canyon, and the ground-level separation di-
188 minishes instead. A direct flow impingement is observed on the windward facade
189 that in turn increases the form drag and the friction factor of the street canyon
190 unit as well.

191 In the skimming flow regime, the upper part of the street canyon is too narrow
192 for persistent entrainment of flow aloft. The impingement on the windward facade
193 does not exist so the LES-calculated friction factor decreases as a result of dom-
194 ination of the weaker shear drag. The aspect ratio of the LES is limited to one.
195 On the other hand, the k - ϵ turbulence modelling results of Liu et al. (2011) show
196 a more uniform friction factor for narrow street canyons. More detailed studies
197 are therefore necessary to examine the flow structure and the resistance for street
198 canyons with $AR > 1$ in order to elucidate the aforementioned difference between
199 LES and k - ϵ turbulence model.

200 It is worth noting the different behaviours of the friction factor calculated by
201 the k - ϵ turbulence model of Liu et al. (2011) and the current LES in the skimming
202 flow regimes of higher aspect ratio. The friction factor calculated by the k - ϵ turbu-
203 lence model converges to around $0.01 \leq f \leq 0.02$. Its LES counterpart, however,

204 is reduced to a lower value that does not show an asymptotic **behaviour**. This
 205 dissimilarity could be a result of the single-length-scale assumption in the k - ϵ tur-
 206 bulence model such that the small-scale intermittent entrainment/de-entrainment
 207 **is** not calculated accurately. Besides, a 2D spatial domain is employed in the k - ϵ
 208 turbulence model while a 3D **domain is used** in the LES. The 3D turbulent motions
 209 **may** lead to different normal stresses that in turn **deviate significantly** from the
 210 **idealized** 2D motions. The modelling accuracy of **the** k - ϵ turbulence model and
 211 LES **has been** compared in **detail** elsewhere (Tominaga and Stathopoulos 2010;
 212 Liu and Chung 2012).

213 3.2 Air Exchange Rate

214 Ventilation of street canyons is **determined from the** air exchange rate (ACH),
 215 which was introduced by Li et al. (2005) and Liu et al. (2005) using **a** k - ϵ turbulence
 216 model and LES, respectively. **The** ACH is calculated by integrating the upward
 217 air velocity normal to the roof level, i.e., it measures the overall volumetric air
 218 removal through the opening gap of a street canyon. A higher ACH thus **favours**
 219 ventilation, carrying aged air from the street canyons to the UBL. For an **idealized**
 220 2D street canyon, the total ACH ($ACH = \overline{ACH} + ACH''$) is partitioned into its
 221 mean

$$\overline{ACH} = \int_{roof} \langle \overline{w}_+ \rangle dA \quad (9)$$

222 and turbulent

$$ACH'' = \int_{roof} \langle w_+'' \rangle dA \quad (10)$$

223 components. Here, the subscript + signifies that only the upward velocity com-
224 ponent is considered and A is the opening gap area of the street canyon. The
225 mean ACH, \overline{ACH} , represents the upward volumetric airflow rate driven by the
226 persistent mean flows. Analogously, the turbulent ACH, ACH'' , carries the aged
227 air upward by the intermittent (upward) turbulent flow. In Fig. 2b, ACH , \overline{ACH} ,
228 and ACH'' exhibit a similar pattern for the range of aspect ratio tested, i.e., the
229 ACH decreases with decreasing aspect ratio in the isolated roughness regime, but
230 decreases with increasing aspect ratio in the wake interference and skimming flow
231 regimes. A broad peak of ACH is observed in the range of $0.0667 \leq AR \leq 0.125$. A
232 wider (narrower) street has a lower (higher) aspect ratio, and thus it is ventilated
233 more (less) efficiently.

234 In the isolated roughness regimes, as discussed previously, the prevailing air
235 masses entrain down to the ground level. The aged air masses are thus purged
236 away from the ground level on the windward side by advection (Liu and Chung
237 2012). A wider street canyon is therefore more favorable for entrainment that in
238 turn improves the ACH. In the skimming flow regime, a primary recirculation is
239 developed inside the street canyon that is isolated from the flow aloft. A dividing
240 streamline (Belcher 2005), bridging the leeward and windward buildings, reduces
241 the persistent entrainment/de-entrainment. The recirculating flow in the street
242 canyon and the flow aloft in the UBL are decoupled, which is similar to the flow
243 over a smooth surface. The ACH is thus largely governed by the intermittent
244 turbulent component ACH'' , leading to a lower level of air exchange. In the wake
245 interference regime, although recirculations persist in the street canyons, they are
246 not isolated from the UBL. The fresh air aloft entrains only the upper part of

247 the street canyons (Cheng et al. 2008). The shallow entrainment, because of its
248 limited vertical and horizontal extents, carries less aged air away from the street
249 canyons by advection. Nonetheless, the air exchange by purging (aged air removal
250 by advection) is more efficient than turbulent transport. Hence, the ACH in the
251 wake interference regime is in-between those of isolated roughness and skimming
252 flow regimes.

253 Taken together, the results observed in the three regimes for the range of aspect
254 ratios tested, clearly show that the ventilation in an idealized 2D street canyon
255 is dominated by turbulent transport. The contribution from \overline{ACH} to the total
256 ACH is rather limited (10% to 20%), we therefore should further examine the
257 role of atmospheric turbulence in the ventilation of urban areas. Cities are mostly
258 compact in design, thus, the roof-level turbulence mainly governs the ventilation
259 performance of street canyons, contributing up to 80% to 90% to the total ACH
260 (in wake interference and skimming flow regimes). Apart from the mean wind,
261 increasing the level of atmospheric turbulence over a city helps remove the ground-
262 level aged air from street canyons in an effective manner.

263 3.3 Pollutant Exchange Rate

264 Similar to its ACH counterpart, the pollutant exchange rate (PCH) is calculated
265 by LES to evaluate the pollutant removal performance of an idealized 2D street
266 canyon. It measures the net amount of total pollutants being removed per unit time
267 from the street canyon to the UBL. Hence, the higher the PCH, the more pollutants
268 can be removed, implying an improved ground-level air quality. Analogous to ACH,

269 the total PCH ($PCH = \overline{PCH} + PCH''$) is comprised of the mean

$$\overline{PCH} = \int_{roof} \langle \bar{w} \rangle \langle \bar{\phi} \rangle dA \quad (11)$$

270 and the turbulent

$$PCH'' = \int_{roof} \langle w'' \phi'' \rangle dA \quad (12)$$

271 components, which are calculated from the vertical pollutant fluxes.

272 Figure 2c depicts the normalized PCH of 2D idealized street canyons as a func-
 273 tion of aspect ratios. Different from its ACH counterpart, because of the unequal
 274 pollutant concentrations across the opening gap of the street canyon, PCHs can
 275 be positive (upward) or negative (downward) that is clearly illustrated in Fig. 2c.
 276 Positive and negative PCHs measure the pollutant removal and re-entrainment,
 277 respectively.

278 In the isolated roughness regime, the PCH is quite uniform for the range of
 279 aspect ratios tested. In view of the persistent entrainment of fresh air from the
 280 UBL down to the street surface, most of the ground-level pollutant, following the
 281 aged air masses, is purged away from the street canyon by the prevailing wind in
 282 the streamwise direction. Therefore, the mean PCH contributes almost 50% to the
 283 total PCH, which is largest among the three flow regimes tested.

284 In the wake interference regime, the PCH behaves differently from its ACH
 285 counterpart. A minimum of total PCH ($= 0.0015\overline{U}\Phi A$) is clearly observed at AR
 286 $= 0.3$, suggesting a substantial drop in pollutant removal in the wake interference
 287 regime for idealized 2D street canyons. The degraded PCH is caused by the shal-
 288 low entrainment of prevailing air which is unable to touch down the ground level
 289 to purge the pollutants away from the street canyons to the UBL by advection.

290 Instead, the entrainment of air carries roof-level pollutants, which are originated
291 from the ground level, downwards into the street canyon. The persistent down-
292 wards pollutant flux, which is illustrated by the negative \overline{PCH} (Fig. 2c), weakens
293 the net (upward) pollutant removal that eventually prolongs the pollutant reten-
294 tion, resulting in the reduced total PCH in the wake interference regime.

295 The PCH decreases with increasing aspect ratio in the skimming flow regime.
296 The mean PCH is negligible (or even negative) so the pollutant removal is domi-
297 nated by the turbulent component PCH'' . Besides, the narrow opening gap area
298 between the leeward and windward buildings are connected by the dividing stream-
299 line. This isolated nature deters mean pollutant removal, leading to the decreasing
300 total PCH.

301 3.4 Consistency with Other Studies

302 Also shown in Fig. 2 are the detailed k - ϵ turbulence model results of Liu et al.
303 (2011). In particular, it provides data for narrow street canyons with aspect ratios
304 up to 2.5 that complements the current LES findings.

305 The friction factors calculated by the k - ϵ turbulence model and the current
306 LES agree well with each other in the range of aspect ratios tested except in the
307 skimming flow regime of high aspect ratios (Fig. 2a). The reasons are detailed
308 previously in Section 3.1.

309 Similar to the friction factor, the ACHs calculated by the k - ϵ turbulence model
310 and the current LES show a discrepancy in the skimming flow regime (Fig. 2b).
311 The LES-calculated turbulent components is lower than that of the k - ϵ turbulence

312 model. Alike the friction factor calculation, this difference is caused by the inher-
313 ent modelling weaknesses of k - ϵ turbulence models handling turbulent transport
314 processes. This finding signifies the dissimilarities between k - ϵ turbulence model
315 and LES, and the associated modelling errors. A similar difference is also found
316 in the PCH in the skimming flow regime.

317 Additional data from literature are compared in Fig. 2c to examine the accu-
318 racy of the current LES. The consistent findings in PCHs from different studies,
319 which are detailed in this section, collectively suggest the pollutant entrainment/de-
320 entrainment mechanism formulated in the previous section.

321 Cai et al. (2008) used another LES model to examine the pollutant removal
322 from street canyons in the skimming flow regime. The pollutant transfer coefficient,
323 which is equivalent to the PCH adopted in this study, was used to compare the
324 pollutant removal behaviours. Their results clearly demonstrated that, in line with
325 our LES findings, the pollutant removal from a 2D idealized street canyon decreases
326 with increasing aspect ratios. We believe that the reasons behind are similar to
327 ours discussed in the previous sections.

328 Barlow and Belcher (2002) and Barlow et al. (2004) conducted naphthalene
329 sublimation experiments over 2D idealized street canyon models in wind tunnels of
330 different sizes. They focused on the pollutant removal behaviours in the skimming
331 flow and wake interference regimes for a range of aspect ratios. In the skimming
332 flow region, the data points are rather sparse that exhibit 20% to 25% of variation
333 for a given aspect ratio. Nevertheless, they fall within the various modelling data
334 sets that collectively suggests the weakened pollutant removal with increasing
335 aspect ratio. Fewer data points were sampled in the wake interference regime,

336 whereas, a mild drop in pollutant removal is observed in the transition across the
337 wake interference and skimming flow regimes. This minimum pollutant exchange
338 rate measured by wind tunnel experiments agrees well with our modelling results
339 using both k - ϵ turbulence model and LES, showing the characteristic pollutant
340 entrainment/de-entrainment for 2D idealized street canyons.

341 3.5 ACH and PCH as Functions of Friction Factor

342 Figure 3 expresses the total ACH ACH and the total PCH PCH as functions of
343 the friction factor f in attempt to determine their correlation. In this preliminary
344 trial, the urban roughness elements are identical in the form of idealized 2D street
345 canyons, their roughness is only adjusted by the `street-canyon` aspect ratios. The
346 total ACH, which is calculated by the k - ϵ turbulence model (Liu et al. 2011) and
347 the current LES, consistently increases with increasing friction factor. Least square
348 fitting of the data points shows that the correlation coefficients for k - ϵ turbulence
349 model ($R^2 = 0.69$) and LES ($R^2 = 0.94$) are high. Hence, the friction factor could
350 be adopted as a parameter to estimate the total ACH or ventilation of a street
351 canyons. On the other hand, least square fitting of the total PCH is less correlated
352 with the friction factor with $R^2 = 0.58$. In particular, the results from the k - ϵ
353 turbulence model shows that the friction factor and PCH is essentially uncorre-
354 lated. It is likely caused by the pollutant entrainment/de-entrainment across the
355 wake interface and skimming flow regimes. This loose correlation as a function of
356 friction factor, similar to that revealed in Liu et al. (2011), also demonstrates the

357 necessity of using ACH and PCH simultaneously to measure the ventilation and
358 pollutant removal of a street canyon.

359 4 Conclusions

360 The large-eddy simulation (LES) with the one-equation subgrid-scale (SGS) model
361 is applied to calculate the wind and pollutant transport in idealized two-dimensional
362 (2D) street canyons with aspect ratios $AR = 0.0667$ and 0.0909 in the isolated
363 roughness regime, 0.25 and 0.3333 in the wake interference regime, and 0.5 , 0.6 ,
364 0.8 , 1 , and 2 in the skimming flow regime. The parameters, including the friction
365 factor f , the air exchange rate (ACH), and the pollutant exchange rate (PCH)
366 are determined to evaluate the drag, the ventilation and the pollutant removal.
367 The friction factor attains its maximum value at $AR = 0.125$ due to the entrain-
368 ment of air from the urban boundary layer (UBL) aloft to the street canyons.
369 The ACH and PCH are compared with the k - ϵ turbulence modelling results of
370 Liu et al. (2011) and consistent findings are obtained. The ACH decreases with
371 increasing aspect ratio, illustrating the more efficient removal of aged air masses
372 from a wider street canyon. However, the improved ventilation does not guaran-
373 tee a more efficient pollutant removal. The minimum PCH appears in the wake
374 interference regime that suggests the possibility of pollutant re-entrainment in 2D
375 street canyons. Furthermore, the turbulent components of ACH and PCH are the
376 key contributors, implying the importance of atmospheric turbulence in the im-
377 provement of city ventilation and street-level air quality. A preliminary study is
378 attempted to examine the parametrizations of the total ACH and PCH using the

379 friction factor. Modelling results show that the flow resistance of flows over street
380 canyons is a potential reliable estimate of the total ACH but not the total PCH.
381 Additional investigations are **required** to improve the PCH estimate.

382 *Acknowledgments*

383 This project is supported by the General Research Fund of the Hong Kong Re-
384 search Grants Council HKU 715209E. The computation is supported in part by a
385 Hong Kong UGC Special Equipment Grant (SEG HKU09). The technical support
386 from Lilian Y.L. Chan, Frankie F.T. Cheung, Tony W.K. Cheung, and W.K. Kwan
387 with **Information Technology Services**, The University of Hong Kong is appreci-
388 ated.

389 **References**

- 390 Ahmad, K., Khare, M. and Chaudhry, K. K. (2005), ‘Wind tunnel simulation studies on dis-
391 persion at urban street canyons and intersections - a review’, *J. Wind Eng. Ind. Aerodyn.*
392 **93**, 697–717.
- 393 Bady, M., Kato, S. and Huang, H. (2008), ‘Towards the application of indoor ventilation
394 efficiency indices to evaluate the air quality of urban areas’, *Build. Environ.* **43**, 1991–
395 2004.
- 396 Barlow, J. F. and Belcher, S. E. (2002), ‘A wind tunnel model for quantifying fluxes in the
397 urban boundary layer’, *Boundary-Layer Meteorol.* **104**, 131–150.
- 398 Barlow, J. F., Harman, I. N. and Belcher, S. E. (2004), ‘Scalar fluxes from urban street canyons.
399 Part I: laboratory simulation’, *Boundary-Layer Meteorol.* **113**, 369–385.
- 400 Belcher, S. E. (2005), ‘Mixing and transport in urban areas’, *Phil. Trans. R. Soc. A.* **363**, 2947–
401 2968.

- 402 Bentham, T. and Britter, R. (2003), ‘Spatially averaged flow within obstacle arrays’, *At-*
403 *mos. Environ.* **37**, 2037–2043.
- 404 Bottema, M. (1997), ‘Urban roughness modelling in relation to pollutant dispersion’, *At-*
405 *mos. Environ.* **31**, 3059–3075.
- 406 Britter, R. and Hanna, S. (2003), ‘Flow and dispersion in urban areas’, *Annu. Rev. Fluid*
407 *Mech.* **35**, 469–496.
- 408 Cai, X. M., Barlow, J. F. and Belcher, S. E. (2008), ‘Dispersion and transfer of passive scalars
409 in and above street canyons - large-eddy simulations’, *Atmos. Environ.* **42**, 5885–5895.
- 410 Cheng, W. C. and Liu, C.-H. (2011a), ‘Large-eddy simulation of flow and pollutant trans-
411 ports in and above two-dimensional idealized street canyons’, *Boundary-Layer Meteorol.*
412 **139**, 411–437.
- 413 Cheng, W. C. and Liu, C.-H. (2011b), ‘Large-eddy simulation of turbulent transports in urban
414 street canyons in different thermal stabilities’, *J. Wind Eng. Ind. Aerodyn.* **99**, 434–442.
- 415 Cheng, W. C., Liu, C.-H. and Leung, D. Y. C. (2008), ‘Computational formulation for the eval-
416 uation of street canyon ventilation and pollutant removal performance’, *Atmos. Environ.*
417 **42**, 9041–9051.
- 418 Chow, V. C. (1959), *Open-channel hydraulic*, first edn, McGraw-Hill Book Co., New York,
419 USA. 680 pp.
- 420 Coceal, O., Thomas, T. G., Castro, I. P. and Belcher, S. E. (2006), ‘Mean flow and turbulence
421 statistics over groups of urban-like cubical obstacles’, *Boundary-Layer Meteorol.* **121**, 491–
422 519.
- 423 Cui, Z. Q., Cai, X. M. and Baker, C. J. (2004), ‘Large-eddy simulation of turbulent flow in a
424 street canyon’, *Q. J. R. Meteorol. Soc.* **130**, 1373–1394.
- 425 Gu, Z.-L., Zhang, Y.-W., Cheng, Y. and Lee, S.-C. (2011), ‘Effect of uneven building layout on
426 air flow and pollutant dispersion in non-uniform street canyons’, *Build. Environ.* **46**, 2657–
427 2665.
- 428 Han, J. C. (1984), ‘Heat transfer and friction in channels with two opposite rib-roughened
429 walls’, *Transactions of the ASME* **106**, 774–782.
- 430 Jiménez, J. (2004), ‘Turbulent flows over rough walls’, *Annu. Rev. Fluid Mech.* **36**, 143–196.

- 431 Kanda, M. (2006), ‘Large-eddy simulations on the effects of surface geometry of building arrays
432 on turbulent organized structures’, *Boundary-Layer Meteorol.* **118**, 151–168.
- 433 Lee, I. Y. and Park, H. M. (1994), ‘Parameterization of the pollutant transport and dispersion
434 in urban street canyons’, *Atmos. Environ.* **28**, 2343–2349.
- 435 Letzel, M. O., Krane, M. and Raasch, S. (2008), ‘High resolution urban large-eddy simulation
436 studies from street canyon to neighbourhood scale’, *Atmos. Environ.* **42**, 8770–8784.
- 437 Li, X. X., Liu, C.-H. and Leung, D. Y. C. (2005), ‘Development of a k - ϵ model for the deter-
438 mination of air exchange rates for street canyons’, *Atmos. Environ.* **39**, 7285–7296.
- 439 Li, X. X., Liu, C.-H. and Leung, D. Y. C. (2009), ‘Numerical investigation of pollutant transport
440 characteristics inside deep urban street canyons’, *Atmos. Environ.* **43**, 2410–2418.
- 441 Liu, C.-H. and Barth, M. C. (2002), ‘Large-eddy simulation of flow and scalar transport in a
442 modeled street canyon’, *J. Appl. Meteorol.* **41**, 660–673.
- 443 Liu, C.-H., Cheng, W. C., Leung, T. C. Y. and Leung, D. Y. C. (2011), ‘On the mechanism of
444 air pollutant re-entrainment in two-dimensional idealized street canyons’, *Atmos. Environ.*
445 **45**, 4763–4769.
- 446 Liu, C.-H. and Chung, T. N. H. (2012), ‘Forced convective heat transfer over ribs at various
447 separation’, *Int. J. Heat Mass Transfer* **55**, 5111–5119.
- 448 Liu, C.-H., Leung, D. Y. C. and Barth, M. C. (2005), ‘On the prediction of air and pollutant
449 exchange rates in street canyons of different aspect ratios using large-eddy simulation’,
450 *Atmos. Environ.* **39**, 1567–1574.
- 451 Michioka, T., Sato, A., Takimoto, H. and Kanda, M. (2011), ‘Large-eddy simulation for the
452 mechanism of pollutant removal from a two-dimensional street canyon’, *Boundary-Layer*
453 *Meteorol.* **138**, 195–213.
- 454 Munson, B. R., Young, D. F. and Okiishi, T. H. (2009), *Fundamentals of Fluid Mechanics*,
455 sixth edn, John Wiley, New York, USA. 725 pp.
- 456 Narita, K. (2007), ‘Experimental study of the transfer velocity for urban surfaces with a water
457 evaporation method’, *Boundary-Layer Meteorol.* **122**, 293–320.
- 458 Oke, T. R. (1988), ‘Street design and urban canopy layer climate’, *Energy and Buildings*
459 **11**, 103–113.

- 460 OpenFOAM (2012), ‘OpenFOAM: The open source CFD toolbox’.
461 <http://www.openfoam.com/>.
- 462 Sini, J. F., Anquetin, S. and Mestayer, P. G. (2005), ‘Pollutant dispersion and thermal effects
463 in urban street canyons’, *Atmos. Environ.* **39**, 1567–1574.
- 464 Smagorinsky, J. (1963), ‘General circulation experiments with the primitive equations I: The
465 basic experiment’, *Mon. Weather Rev.* **91**, 99–165.
- 466 Tominaga, Y. and Stathopoulos, T. (2010), ‘Numerical simulation of dispersion around an
467 isolated cubic building: Model evaluation of RANS and LES’, *Build. Environ.* **45**, 2231–
468 2239.
- 469 Vardoulakis, S., Fisher, B.-E. and Pericleous, K. Gonzalez-Flesca, N. (2003), ‘Modelling air
470 quality in street canyons: a review’, *Atmos. Environ.* **37**, 155–182.

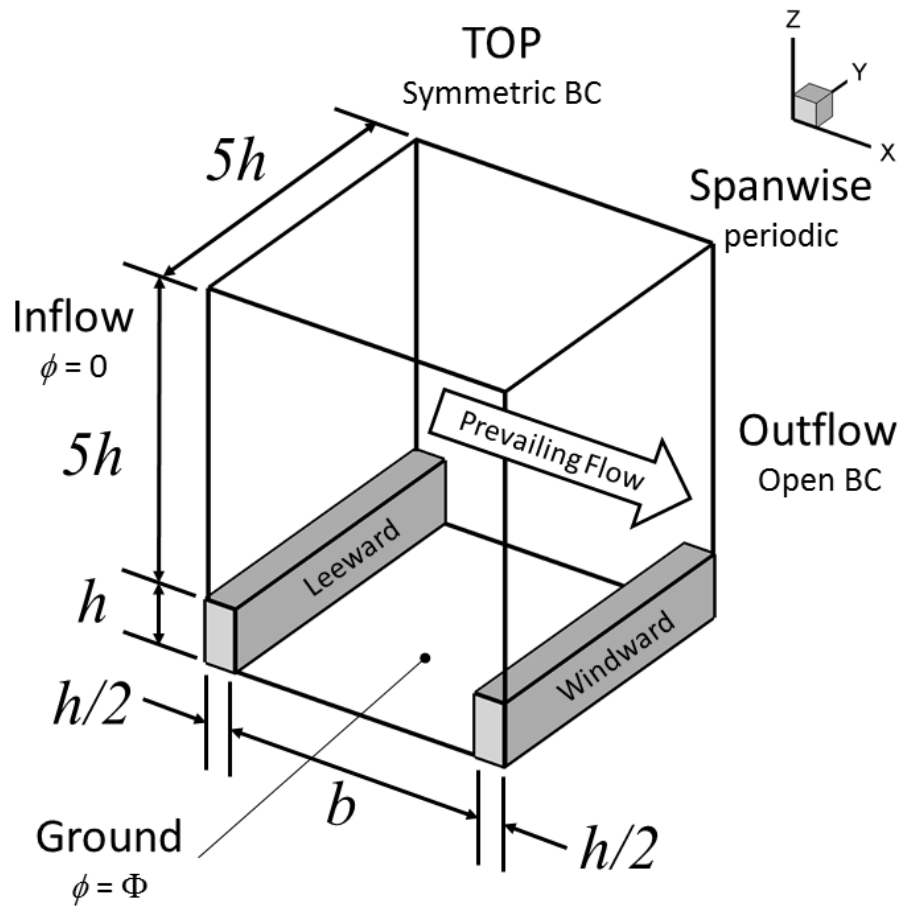


Fig. 1 Three-dimensional LES computational domain.

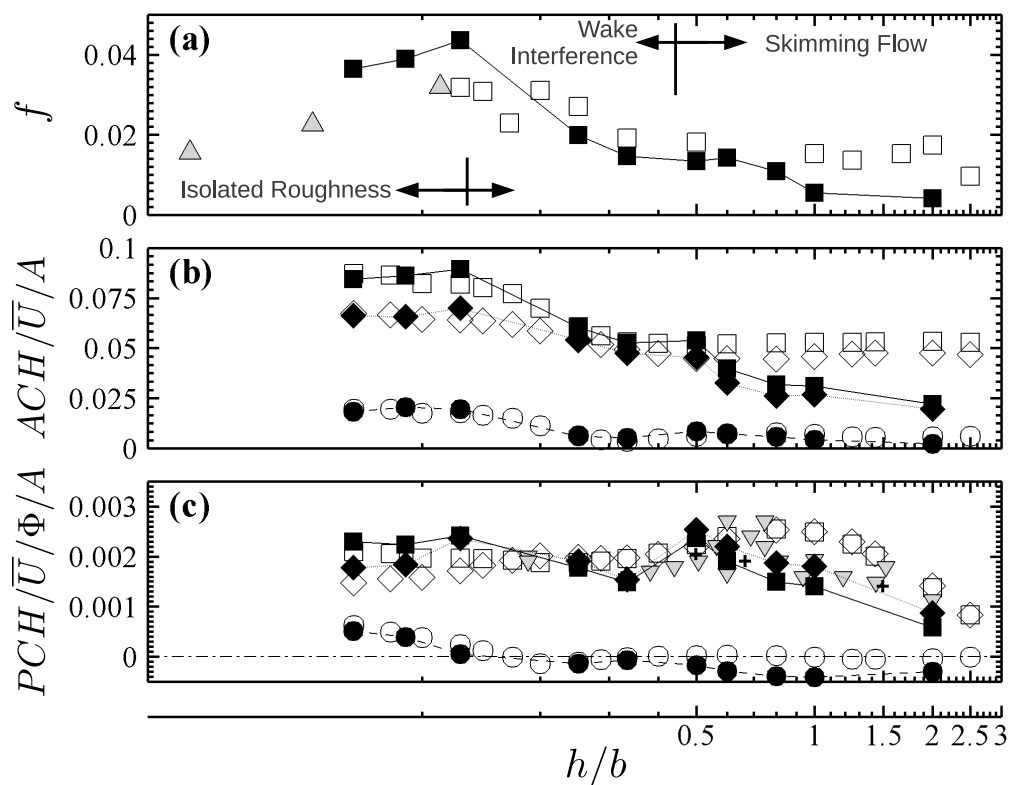


Fig. 2 (a). Friction factor f , (b). air exchange rate ACH , and (c). pollutant exchange rate PCH for idealized 2D street canyons of different building-height-to-street-width (aspect) ratio h/b calculated by $k-\epsilon$ turbulence model (empty symbols, Liu et al. 2011) and the current LES (filled symbols). \circ : Mean component, \diamond : turbulent component, and \square : total quantity. Also shown in shaded symbols are the experimental and numerical data available in literature. Δ : friction factor measurements of Han (1984), ∇ : naphthalene evaporation measurements of Barlow and Belcher (2002) and Barlow et al. (2004), and $+$: LES calculation of Cai et al. (2008). The dash-dotted line represents zero PCH. The flow regime is defined based on the current LES results instead of that stated in Oke (1988).

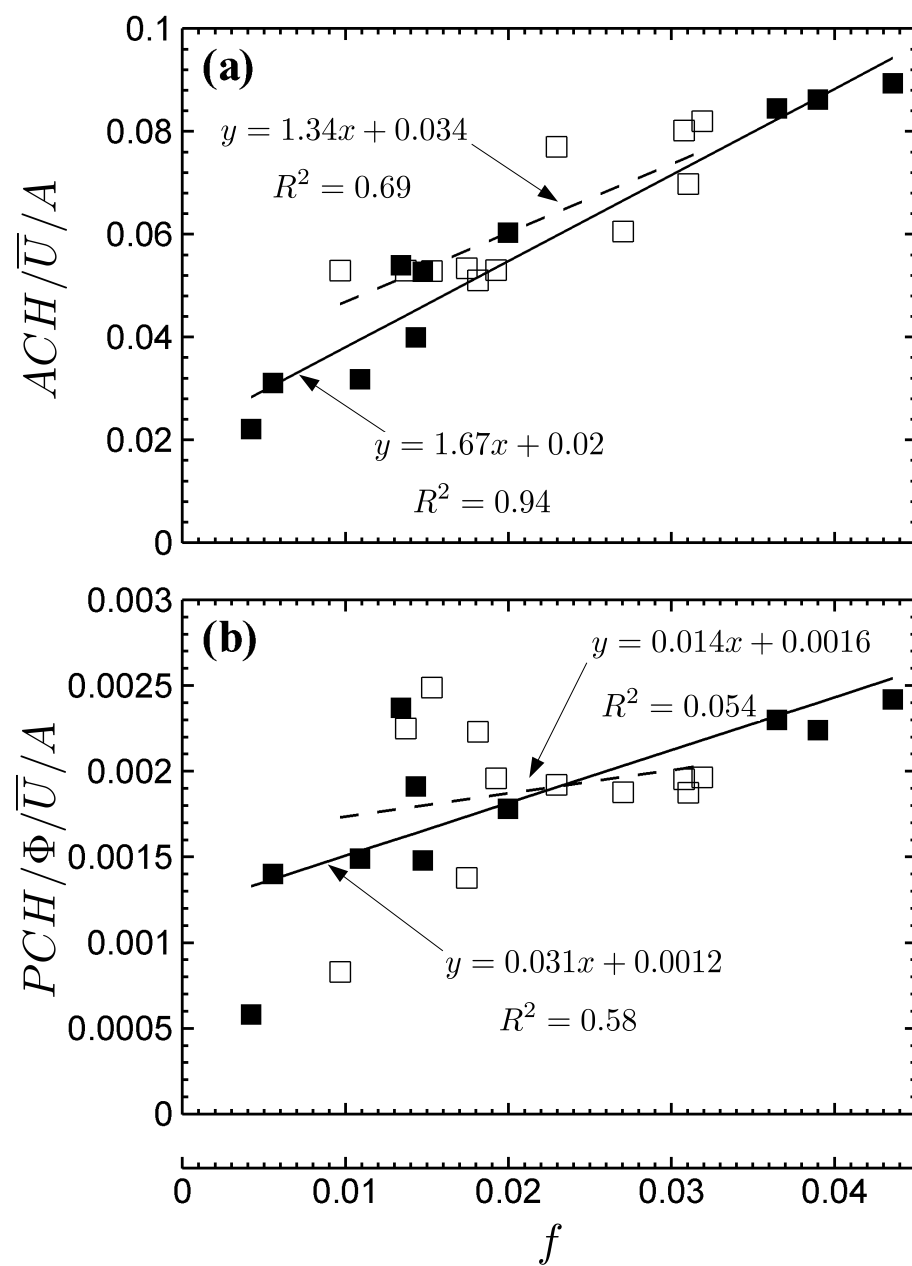


Fig. 3 (a). Air exchange rate ACH and (b). pollutant exchange rate PCH plotted as functions of friction factor f . Also shown are the linear regressions for the modelling results. ■ and —: LES results, and □ and - - - - -: $k-\epsilon$ turbulence model results.